F. Andreola, M.I. Martín, A.M. Ferrari, I. Lancellotti, F Bondioli, J.Ma. Rincón, M. Romero, L. Barbieri, Technological properties of glass-ceramic tiles obtained using rice husk ash as silica precursor. *Ceramics International* Volume 39, Issue 5, July 2013, Pages 5427–5435; doi:10.1016/j.ceramint.2012.12.050

Technological properties of glass-ceramic tiles obtained using rice husk ash as silica precursor

F. Andreola[a] , M.I. Martín[c], A.M. Ferrari[b], I. Lancellotti[a], F Bondioli[a], J.Ma. Rincón[c], M. Romero[c], L. Barbieri[a]

a Department of Engineering "Enzo Ferrari", University of Modena and Reggio Emilia, Via Vignolese 905, 41125 Modena, Italy
b Department of Science and Methods of Engineering, University of Modena and Reggio Emilia, Via Amendola 2, 42100 Reggio Emilia, Italy
c Group of Glassy and Ceramic Materials, Department of Construction, Eduardo Torroja Institute for Construction Science (IETcc) CSIC, Serrano Galvache 4, 28033 Madrid, Spain

Abstract

This paper reports the results of a study focused on the obtainment of glass-ceramic by using rice husk ash (RHA) as silica precursor. RHA is a by-product generated in biomass plants using rice husk as fuel for kilns or in the rice mills to generate steam for the parboiling process. Worldwide, it is annually produced about 132 Mt of rice husk, which gives rise to a production of 33 Mt/year of RHA. Glass-ceramic tiles were produced by a sinter-crystallization process using a glassy frit formulated in the $MgO–Al_2O_3$-SiO_2 composition system. The realized glass-ceramics were studied according to ISO rules for sintering and technological properties (water absorption, apparent density, bending strength, Young's modulus, deep abrasion, Mohs hardness). To complete the investigation crystalline phase formation and microstructural characterization of the glass-ceramic materials was carried out using X-ray diffraction (XRD) and scanning electron microscopy (SEM). Finally, chemical durability tests on parent glass and derived glass-ceramics were performed. The results obtained showed that it is possible to use RHA to produce glass-ceramic tiles by a sinter-crystallization process, obtaining nepheline ($Na_2O*Al_2O_3*SiO_2$) as main crystalline phase and forsterite ($2MgO*SiO_2$) at 900 °C. Regarding technological features, the sintered materials showed bending strength values and Mohs hardness higher with respect to commercial glass-ceramics like NeopariesR. Other properties as water absorption (0.5%) allowed to classify these materials into the Group BIa characteristic of high sintered ceramic tiles according to European Standard rule.

Keywords

A. Sintering; B. Microstructure final; C. Mechanical properties; D. Traditional ceramics

F. Andreola, M.I. Martín, A.M. Ferrari, I. Lancellotti, F Bondioli, J.Ma. Rincón, M. Romero, L. Barbieri, Technological properties of glass-ceramic tiles obtained using rice husk ash as silica precursor. *Ceramics International* Volume 39, Issue 5, July 2013, Pages 5427–5435; doi:10.1016/j.ceramint.2012.12.050

1. Introduction

Rice cultivation is the principal activity and source of income for millions of households around the globe, and several countries of Asia and Africa are highly dependent on rice as a source of foreign exchange earnings and government revenue. Rice is the second largest produced cereal in the world. At the beginning of the 1990s, annual production was around 350 million tons and in 2008 it has reached 661 million tons [1]. The first step of the production process, after the rice harvest, is the milling process that generates a by-product known as husk (a low-density residue of the process) that surrounds the paddy grain. During milling of paddy about 80% of weight is received as rice, broken rice and bran while the remaining 20% is received as husk. Consequently, in 2008 the world rice production has also generated 132 million tons of rice husks. Disposal of rice husk is, therefore, an important issue in those Countries that cultivate large quantities of rice (i.e. East and South-East Asia). Even if there are some uses for rice husk, it is still often considered a waste product and therefore often either burned outdoor or dumped on wasteland. Rice husk occupies large areas, has a very low nutritional value and, as it takes very long time to decompose, it is not appropriate for composting or manure. One effective method used today to reduce the rice husk accumulation is to use it as fuel for kilns to produce bricks and other clay products or in the rice mills to generate steam for the parboiling process. Rice husk contains about 75% organic volatile matter, thus 25% of the weight of this husk is converted into ash during the firing process. The latter, known as rice husk ash (RHA), is an ash product with an unburned carbon percentage (∼10%), which contains around 85%–90% of amorphous silica. This means that every 1000 kg of milled paddy, about 220 kg (22%) of husk is produced, and when this husk is burnt, about 55 kg (25%) of RHA is generated. Using this data, the total global rice husk ash production could be as high as 33 million tons per year [2] and [3].

The presence of silica in RHA was known since 1938 [4] and an extensive search of the literature highlighted many uses of RHA. Two main industrial uses were identified: as an insulator in the steel industry and as a pozzolanic material in the cement industry [5] and [6]. RHA is used by the steel industry in the production of high quality flat steel. In fact, RHA is an excellent insulator, having low thermal conductivity, high melting point, low bulk density and high porosity. It is this insulating property that makes it an excellent ‘tundish powder’ that prevents rapid cooling of the steel and ensures uniform solidification in the continuous casting process. In addition, substantial research was carried out on its use in the manufacture of concrete. In particular, there are two areas in which RHA is used: in the manufacture of low cost

building blocks, and in the production of high quality cement. The addition of RHA to cement enhances the cement properties. In particular its addition to Portland cement not only improves the early strength of concrete, but also leads to the formation of a calcium silicate hydrate gel around the cement particles, which becomes highly dense and less porous. This may increase the strength of concrete against cracking. In general, concrete made with Portland cement containing RHA has a higher compressive strength.

Considering the ceramic sector, in these last years, different studies were performed in order to valorize this type of waste as silica precursor; in particular RHA was used for whiteware [7] and ceramic production [8] and [9], synthesis of pigments [10] and [11] and glaze production [12] and [13]. In fact, in this field the use of this waste as silica precursor can be seen as a prevention of waste produced during the extraction of raw materials according to the environmental sustainability criteria.

Regarding glass-ceramics, Naskar et al. used this agricultural waste material to successfully synthesize lithium aluminum silicate (LAS) powders in the form of β-eucryptite (LA2S) and β-spodumene (LA4S) [14].

Among the different glass ceramic system, the nepheline-based glass-ceramics are characterized by high mechanical strength and impact resistance and thus they are very attractive for the potential use such as in microwave ovens [15] and dental applications[16] and [17].

Nepheline glass-ceramics are usually prepared from high purity proportions of pure chemicals and by the addition of different nucleating agents, such as TiO_2, Cr_2O_3, ZrO_2 or LiF to promote crystallization [18] and [19]. They can be also prepared from cheaper raw materials such as wastes because the glass-ceramic process was established as a suitable way to valorize mining and industrialwastes [20] and [21], including fly ash from incineration [22] and [23] and thermal power plants [24] and [25], wastes from hydrometallurgical processing plants [26], residual glass fibers from polyester matrix composites [27], among others wastes.

Forsterite has a sintering temperature of about 1500 °C, which is too high and imposes limits to its application. Many efforts were made to improve the workability of forsterite, including the reduction of the firing temperature by alumina addition [28] or using low melting point glasses [29]. Another way to produce forsterite materials at lower temperatures could be through the glass-ceramic process. Indeed, several investigations report the devitrification of forsterite as secondary crystalline phase in glass-ceramics belonging to different composition systems. In particular, Demirci and Günay [30] studied the crystallization behavior of cordierite glass-

ceramics containing B_2O_3 boron oxide. They concluded that crystallization started at 950 °C after 1 h of heat treatment thus obtaining indialite ($Mg_2Al_4Si_5O_{18}$) as primary phase, followed by forsterite (Mg_2SiO_4) as secondary one with contents of around 89.2% and 10.8% respectively.

In a recent work [31], the authors demonstrated the feasibility of producing nepheline-forsterite-based glasses with the use of rice husk ash (RHA) as the main raw material (~46 wt%). The glass-ceramics were produced by a sintering process of a glassy frit formulated in the $MgO–Al_2O_3–SiO_2$ based system with the addition of B_2O_3 and Na_2O to facilitate the melting and pouring processes and Al_2O_3 and MgO to favor the fosterite crystallization. These glasses lead to glass-ceramics that combine the beneficial properties associated with both the forsterite and nepheline crystalline phases.

Starting from these researches, the aim of this work is to study the effect of sintering temperature on the densification process and the microstructure and mineralogical composition of the nepheline–fosterite glass-ceramic tiles obtained from RHA in order to determine the correlation with their physical, chemical and technological properties.

2. Materials and methods

The rice husk ash (RHA) used in this work comes from a plant producing parboiled rice (Garibaldi 1889, Colussi S.p.A., Milan, Italia). The as received RHA contained about 8% of unburned organic carbon. Prior to its use, the ash was treated at 500 °C and sieved to a particle size <250 μm. A glass (hereafter designed RHA glass) belonging to the $SiO_2–Al_2O_3–MgO$ base system were formulated with the addition of B_2O_3 and Na_2O to facilitate the melting process and Al_2O_3 and MgO to favor the fosterite crystallization. The chemical reagents used, all A.R. quality, were Al_2O_3, MgO, B_2O_3 and Na_2CO_3. The components (46.52 wt% calcined ash, 13.84 wt% Al_2O_3, 13.16 wt% MgO, 22.17 wt% Na_2CO_3 and 4.33 wt% B_2O_3) were mixed for 30 min in a blender (TURBULA) to get a homogeneous mixture. The batch was placed in an aluminosilicate crucible and was heated at 10 °C/min in an electric furnace up to 1450 °C. After a holding time of 120 min at the melting temperature, the melt was quenched into water producing a glass frit.

The chemical composition of the RHA and glass frit was determined by X-ray fluorescence (XRF) (Thermo Scientific model ARL ADVANT′XP) and inductively coupled plasma spectroscopy (ICP) (Varian model Liberty 200), respectively.

2.1. Sample preparation

In a previous paper, it was pointed out that the devitrification process of RHA glass went through a surface crystallization mechanism [31]. Thus, the most effective method for manufacturing this glass-ceramics materials from RHA glass is by a sinter-crystallization process, which involves the sintering and subsequent crystallization of powdered glass. Therefore, the study below reported regards samples prepared by pressing glass powders with a grain size lower than 63 μm.

Powdered RHA glass was moistened by spraying distilled water (2 wt%). Glass compacts (1×1 cm^2) were shaped by uniaxial pressing (Nannetti S hydraulic press) at 40 MPa in a steel die. Moreover, in order to evaluate the physical and technological properties, square laboratory tiles (5×5 cm^2) were prepared using clay (5 wt%) as binder to prevent the formation of defects during firing.

In order to study the sintering-crystallization process, glass compacts were thermally treated at different temperatures (650–1000 °C) for several times (2–60 min). Samples were successively cooled to room temperature. Furthermore, in order to evaluate the physical and technological properties of the glass-ceramic, the obtained tiles were fired in an electrical kiln at different maximum temperatures (750, 800, 900 and 1000 °C) and soaking time of 40 min.

2.2. Sample characterization (glass-ceramic)

The evaluation of the amorphous nature of the melted glass and the crystalline phases developed during the thermal treatments was performed by X-ray diffraction (XRD) (Philips model X ‘PERT MPD) with Ni-filtered Cu Kα radiation operating at 40 mA and 40 kV. For the qualitative analysis, data were recorded in the 3–75° 2θ range (step size 0.02° and 0.5 s counting time for each step). Moreover, the quantitative study was performed by combined Rietveld and Reference Intensity Ratio (R.I.R) methods. Data were recorded in the 5–140° 2θ range (step size 0.02° and 6 s counting time for each step). The initial crystal structure parameters of crystalline phases were taken from ICSD data base. The phase fractions extracted by the Rietveld-R.I.R. refinements, using the GSAS software and EXPGUI as graphical interface [32] and [33] were rescaled on the basis of the absolute weight of corundum originally added to the mixtures as an internal standard, and therefore internally renormalized. The background was successfully fitted with a Chebyshev function with a variable number of coefficients depending on its complexity. The peak profiles were modeled using a pseudo-Voigt function with one Gaussian and one Lorentzian coefficient. Lattice constants, phase fractions and coefficients corresponding to sample displacement and asymmetry were also refined.

The microstructural analysis of glass-ceramic materials was performed by field emission scanning electron microscopy (FESEM) (JEOL model JSM 6500 F) using an accelerate voltage of 20 kV. SEM specimens were polished using 6, 3 and 1 μm diamond pastes after grinding with silicon carbide paper and water. The polished surfaces were etched for 10 s in a 5 vol% HF solution, washed ultrasonically with distilled water and ethylic alcohol, dried and subsequently coated with Au–Pd in a Balzers SCD 050 sputter.

The water absorption was measured according to EN ISO 10545-3, which involves drying the test specimens to constant mass (D), boiling in distilled water for 2 h. The mass of the samples were weighted both before and after the water immersion to determine the percentage of water absorption. The test was carried out on ten representative specimens. Water absorption, WA (%), expresses the relationship of the mass of water absorbed to the mass of the dry specimen as follows:

$$WA=[(M-D)/D]\times 100 \quad (1)$$

where *M* is the mass of wet specimen and D is the mass of dry specimen

The apparent (*ρa*), skeleton (*ρs*), and absolute (*ρas*), densities of the glass-ceramic samples were determined and the results were used to calculate total (PT), closed (PC), and open (PO) porosity:

$$P_T = 100 \times \frac{\rho-\rho_a}{\rho_{as}} \quad (2)$$

$$P_C = 100 \times \frac{\rho-\rho_s}{\rho_{as}} \quad (3)$$

$$P_O = 100 \times \frac{\rho_s-\rho_a}{\rho_{as}} \quad (4)$$

ρ_a was estimated by an envelope density analyzer (GeoPyc 1360, Micromeritics) using a dry-flow medium, while ρ_s and ρ_{as} by gas (He) pycnometer (AccyPy1330, Micromeritic). Samples "ad hoc" were prepared for the tests: (ρ_a): cube pieces (1×1×1 cm^3), (ρ_s) irregular pieces with size below 4 mm and (ρ_{as}) powders below 26 μm [34].

Bending strength was measured according to UNE-EN 843-1:2006 in an electronic universal tester (Servosis model ME-402/01) on ten test pieces (50×10×3 mm^3) by a three point loading test with a span of 32 mm and a crosshead speed of 1 mm/min.

Young's modulus (*E*), shear modulus (*G*) and Poisson's ratio (ν) were determined by non-destructive resonance frequency testing (Lemmens Grindosonic Electronika MK5, LTD

analyzer). The elastic modulus values were calculated using dimensions, shape and weight data samples running EMOD software program. In order to meet the ASTM 1259 testing method for dynamic elastic modulus the samples were cut using a saw cutting machine (49×15×3 mm^3) for matching the following rules: width/length ≤0.33; width/thickness ≤10. The average value and standard deviation reported were calculated on 5 tests samples [35].

Mohs hardness was estimated using a laboratory kit (Gabbrielli srl) composed by 10 readily available minerals (talc, gypsum, calcite, fluorite, apatite, feldspar, quartz, topaz, corundum, diamond). The Mohs scale is based on these minerals, everyone has a specific number, raging 1–10.

The deep-abrasion resistance of all samples was measured according to the ISO 10545.6 standard for unglazed ceramic tiles using an abrasimeter (Ceramic Instruments, model AP/87). F80 aluminum oxide powder (ISO 8486-1) was used as abrasive. The glass-ceramic samples were pressed by a 40.2 N normal load against a Fe360A steel wheel, rotating at 75 rpm, with a tangential flow of alumina particles (mean diameter ≈180 μm) FEPA 80 (1 g of alumina per wheel revolution) for 150 revolutions. The resistance to deep abrasion is expressed as volume V (mm^3) of the material removed.

$$V = \left(\frac{\pi\alpha}{180} - \sin\alpha\right)\frac{hd^2}{8} \tag{5}$$

where α is angle, h is the thickness of disk, in mm, d is the diameter of disk, in mm and $L$is the length of the mark, in mm.

$$\sin(0.5\alpha) = L/d$$

The volume values of material removed were obtained by interpolation of L and V tabulated data [36].

Following ISO 719 rules, the durability tests in water were also conducted. For the tests 2 g of powdered glass ceramic samples, 250–500 μm particle size, were disposed in 50 ml of bi-distilled water, all immersed in a boiling water bath for 1 h. Quantitative analysis of alkali release (Na^+, K^+) was conducted by ICP (inductively coupled plasma Varian Liberty 200) on the solutions.

3. Results and discussion

The chemical composition of both the rice husk ash (RHA) after the thermal treatment at 500 °C and the obtained RHA glass are reported in Table 1. The major component of the ash is

F. Andreola, M.I. Martín, A.M. Ferrari, I. Lancellotti, F Bondioli, J.Ma. Rincón, M. Romero, L. Barbieri, Technological properties of glass-ceramic tiles obtained using rice husk ash as silica precursor. *Ceramics International* Volume 39, Issue 5, July 2013, Pages 5427–5435; doi:10.1016/j.ceramint.2012.12.050

very pure SiO_2 (~91 wt%) and among the minor components P_2O_5 shows the highest concentration (3.62 wt%). Other oxides as alkalines and alkaline earths are in percentages lower than 1.60 wt%. The chromophore oxides as Fe_2O_3 and TiO_2, that can influence the color developed in a ceramic matrix, are present only as traces. These results allowed to orient the research towards the use of this residue as silica precursor for glass-ceramics. The SiO_2–Al_2O_3–MgO–Na_2O system was chosen in order to obtain glass-ceramics with properties suitable for use as building materials.

Table 1. Chemical composition (oxide wt%) of RHA after the thermal treatment at 500 °C and RHA glass.

Oxide (wt%)	RHA	RHA glass
SiO_2	90.75	44.18
Al_2O_3	0.06	18.22
CaO	1.20	0.68
MgO	0.84	12.24
K_2O	1.56	1.86
Fe_2O_3	0.16	0.06
Na_2O	–	17.06
B_2O_3	–	5.21
P_2O_5	3.62	0.48
TiO_2	0.03	–
ZnO	0.01	–
SO_3	1.62	–
MnO	0.16	–

The mineralogical results obtained by the Rietveld-RIR analysis showed that RHA is mainly constituted by amorphous silica (77.2 (2) wt%) and by tridymite (5.6(2) wt%) and cristobalite low (17.2(2) wt%) as crystalline phases [13].

The quantitative results underline that, as reported by Ibrahim [37], the thermal treatment performed on the rice to obtain the parboiled type favors the nucleation and growth of cristobalite phase which, in general, starts to appear at 900 °C [38]. The presence of tridymite, instead, is governed by the kind and amount of impurities [39]. Regarding RHA glass, SiO_2, Al_2O_3, Na_2O_3 and MgO are the main components in its composition.

The T–T–T (Time–Temperature–Transformation) curves define the combinations of time and temperature needed for the onset of crystallization. From the TTT results reported elsewhere [31] it was decided to use the same soaking time for all thermal treatments in order to

ensure that the crystallization occurred of the crystallization occurred. So for the technological tests the samples were fired at different temperatures (750, 800, 900, 1000 °C) with a soaking time of 40 min.

The qualitative XRD study carried out on all samples after heat treatment showed that RHA glass devitrification leads to a glass-ceramic material mainly composed of nepheline ($Na_2O{\cdot}Al_2O_3{\cdot}2SiO_2$) in the 700–1000 °C temperature range while forsterite ($2MgO{\cdot}SiO_2$) appeared starting from 750 °C. In order to better understand the thermal behavior of the system, quantitative analysis were performed on the nepheline and forsterite crystalline phases parameters taken from ICSD data base (nepheline ICSD #201572 and forsterite ICSD #50080) by refining, in particular, the site occupancy factors for the Na and K atoms in nepheline phase (Table 2). The Rietveld-R.I.R results confirm that devetrification begins at 700 °C with nepheline crystallization. The highest amount of nepheline is developed at 750 °C where reach 45%.

Table 2. Results of Rietveld-R.I.R quantitative analysis (wt%), agreement indices (Rwp, Rp) and the additional statistical indicator ($\chi 2$) for the glass-ceramics obtained at different temperatures (soaking time 40 min.).

T (°C)	Nepheline (wt%)	Forsterite (wt%)	Glassy phase	$\chi 2$	Rwp	Rp
700	1.2(1)	–	98.8(2)	0.691	0.526	0.391
750	45.5(1)	4.9(1)	49.6(4)	1.455	0.639	0.485
800	43.1(1)	11.6(1)	45.3(3)	1.429	0.633	0.481
900	42.1(1)	11.3(3)	46.6(4)	1.403	0.628	0.474
1000	40.1(1)	11.7(2)	48.2(4)	1.470	0.638	0.483

Fig. 1 shows the Rietveld-RIR refinement for the sample fired at 900 °C where the amount of nepheline is decreasing to 42% and the amount of forsterite reaches the maximum value of about 11%. Increasing the temperature (1000 °C), the nepheline starts to melt, as confirmed by the increase of the glassy phase (48%), while the amount of fosterite is constant (~11%).

F. Andreola, M.I. Martín, A.M. Ferrari, I. Lancellotti, F Bondioli, J.Ma. Rincón, M. Romero, L. Barbieri, Technological properties of glass-ceramic tiles obtained using rice husk ash as silica precursor. *Ceramics International* Volume 39, Issue 5, July 2013, Pages 5427–5435; doi:10.1016/j.ceramint.2012.12.050

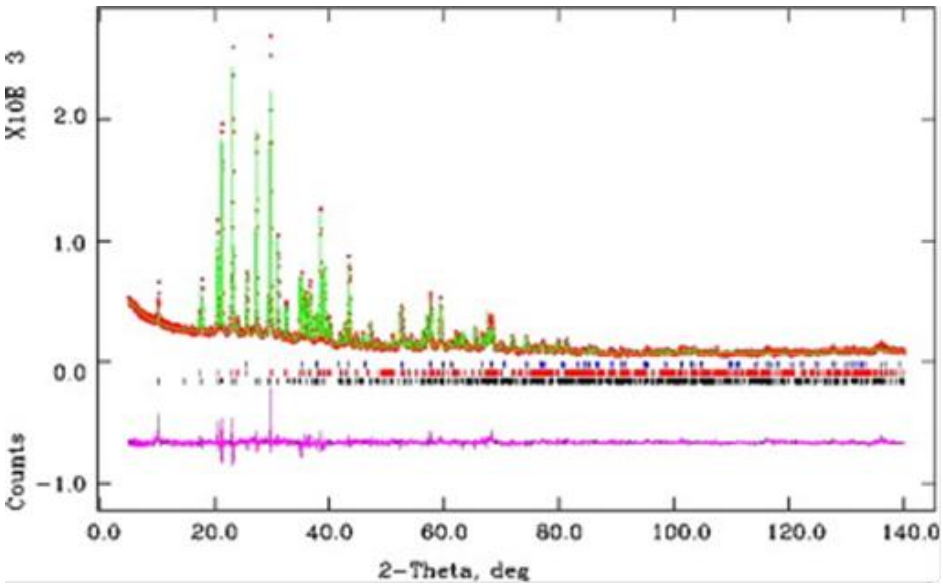

Fig. 1. Observed (crosses), calculated (continuous line), and difference curve from the Rietveld R.I.R refinement of the sample treated at 900 °C in air. Markers representing the phase reflections correspond to corundum, forsterite and nepheline (from top to bottom).

Regarding the densification study, Table 3 reports the measured densities and the calculated porosities as a function of the thermal treatments. On the basis of literature density values for nepheline (2.60 g/cm^3) and fosterite crystalline phases (3.27 g/cm^3), the obtained samples show a positive trend of absolute density values with the increase of temperature. The experimental values are close to nepheline density and in agreement with Rietveld analysis that underlines that nepheline neopheline is the main crystalline phase. Regarding apparent density, the increase of the sintered material densities by increasing the sintering temperature up to 900 °C is in accordance with the viscous sintering theory, which correlates the temperature dependence of the sintering process to the temperature dependence of the glassy phase viscosity. On the other hand, the sample treated at 1000 °C shows a decrease of apparent density due to a bloating effect. In fact, closed porosity strongly increases as the temperature is increased reaching 22 wt% for a thermal treatment at 1000 °C. The bloating phenomenon, in the form of a high concentration of coarse pores, takes place by retention of gas within the mass when a considerable quantity of glass (~50%) of adequate viscosity is present.

Table 3. The measured apparent, ρa, skeleton, ρs, and absolute, ρas, densities and the calculated total (PT), open (PO) and closed (PC) porosities of glass-ceramics obtained at different temperatures (soaking time 40 min.).

Temperature (°C)	Apparent density ρa (g/cm^3)	Skeleton density ρs (g/cm^3)	Absolute density ρas (g/cm^3)	Closed porosity (%)	Open porosity (%)	Total porosity (%)
750	2.091±0.016	2.593±0.002	2.625±0.002	1.966	18.981	20.948
800	2.248±0.009	2.434±0.001	2.636±0.002	7.666	7.070	14.736
900	2.262±0.006	2.394±0.001	2.640±0.002	9.306	5.034	14.340
1000	1.973±0.009	2.054±0.001	2.646±0.002	22.364	3.069	25.433

The open porosity decreases with the increase of temperature indicating a densification process, accelerated by the formation of liquid phase. Finally, concerning the total porosity, the lowest value is obtained at 900 °C in accordance with the described behaviors.

Table 4 shows the technological properties of the glass-ceramic tiles obtained from RHA glass after different thermal treatments.

Table 4. Sintering and technological properties: water absorption (WA%), Bending strength (BS), Young's modulus (E), Shear modulus (G), Poisson ratio (μ), Mohs hardness, Deep abrasion for the glass-ceramics obtained at different temperatures (soaking time 40 min).

Temperature (°C)	750	800	900	1000
Water absorption (WA%)	3.41	2.82	0.41	0.29
Bending strength (MPa)	34±3	35±2	39±3	24±3
Young's mod. (GPa)	42.83±1.59	60.50±1.70	60.85±2.03	46.77±1.56
Shear modulus (GPa)	18.73±0.55	20.50±0.70	23.08±0.60	16.84±0.45
Poisson ratio (ν)	0.14	0.24	0.20	0.30
Mohs hardness	6–7	6–7	8–9	8–9
Deep abrasion (mm^3)	352	207	205	221

Water absorption is directly related to open porosity and therefore, this property decreases with increasing temperature so that from 900 °C water absorption values lower than 0.5% are reached. The bending strength increases slightly with temperature due to the higher sintering

degree of the tiles and the development of crystalline phases. However, an excess of glassy phase and an increase of closed porosity, originated by the partial dissolution of nepheline crystals, causes a fall of this property for temperatures exceeding 900 °C. At 900 °C, the sintered bodies show a bending strength value of 39 MPa, which is similar to commercial glass-ceramics like Neoparies® which has a bending strength value of 41 MPa [40]. This commercial product is the most significant glass-ceramic tile produced on a large scale as a building material for building applications in both interior and exterior walls.

Besides, the material fired in these conditions (900 °C, 40 min) showed a water absorption value determined followed EN ISO 10545-3 rules [41] less than 0.5% (Table 4) typical value of high sintered ceramic products as porcelain stoneware tiles.

In according to the European Standard ISO 13006, the products with water absorption ≤0.5% belongs to the BIa group (high sintered ceramic tiles as porcelain stoneware tile) [41].

The effects of sintering temperature on the other mechanical properties (Young's modulus, Mohs hardness and deep abrasion) are in accordance to the trend showed by bending strength (Table 4). The improvement of the mechanical properties and density of the fired samples with increasing temperature up to 900 °C is confirmed. However, at 1000 °C an overall reduction in bending strength, Young's modulus and wear resistance was observed.

The results of Young's modulus obtained for the samples fired at 900 °C (E=61 GPa) compared to other glass ceramics in literature, confirmed similar properties [42]. The ratio of Young's modulus to bending strength was of the order of 1000 in agreement with that of most ceramic materials [43]. The differences between the E experimental values obtained with respect to the theoretical values for the single crystalline phases, namely 150 GPa for forsterite and 85 GPa for nepheline, are associated to both the high amount of glassy phase and the porosity present in the materials.

It is known that, the Young's modulus of material depend on phase constitution and the shape and distribution of any porosity. All elastic properties are influenced by the level of porosity since pores act as a second phase of a zero modulus. The porosity reduces Young's modulus according to numerous equations found in the literature, for example, the following dependence of E on porosity (P) was proposed by Boccaccini and Boccaccini: $E(P)=E0(1-P2/3)s$, where E(P) and E0 are the Young's modulus of the porous body and of the dense material (pore-free) respectively and s is a factor depending on pore shape and orientation [44].

The Poisson's ratio (ν) of a stable, isotropic, linear and elastic material cannot be less than −1.0 not greater than 0.5 due to the requirement that Young's modulus (E), shear modulus (G) and bulk modulus have positive values [44]. In our study the samples obtained have Poisson's ratio values ranging between 0.14 and 0.30 in agreement with most ceramics [45].

The hardness of samples was measured by the Mohs scale by finding the hardest and/or the softest material that can scratch the given material. From the hardness measures it was possible to note that this kind of glass ceramic independently of the sintering temperature shows hardness values higher than Neoparies® glass-ceramic (5.5) [40]. The values obtained for samples up to 800 °C are similar to natural stones and ceramic rocks (quartz). On the contrary, the glass-ceramic obtained after thermal treatment at 900 °C shows hardness surface values similar to high sintered ceramic tiles (porcelain stoneware).

For the abrasion tests the more the sample is resistant, the smaller is the volume of the material removed. From data reported in Table 4 it is possible to observe a decreasing trend up to 900 °C in agreement with the other mechanical properties. The dry particles abrasion resistance of these glass-ceramics is very poor compared to the one presented by traditional ceramic tiles for floor covering. The abrasion volume removed for all samples was higher than 175 mm3 limit value suggested by the ISO rule. This result suggests the use of glass ceramics obtained as wall covering tile where abrasion resistance is less important.

From these results it is possible to evidence that the best conditions for obtain sintered samples was 900 °C, 40 min. These results can be explained on the basis of FESEM analysis (Fig. 2, Fig. 3 and Fig. 4). At the early stages of crystal growth (700 °C), the glass-ceramic shows a typical coast-and-island microstructure [46] characterized by crystals conglomerates forming a coast, while the glassy phase enclosed by the crystals appears like islands showing an important extent of open porosity, in agreement with the porosity values calculated (Fig. 2a and b). As the temperature increases (800 °C), the open porosity is reduced but simultaneously close porosity consisting of rounded pores increases (Fig. 3). Most significant microstructural and mineralogical changes are observed after the thermal treatment at 900 °C. The percentage of nepheline phase decreases (45–42%) and simultaneously, the amount of amorphous phase reaches 48%. The treatment at 900 °C also leads to a new change in the morphology of nepheline crystals, which appear as hexagonal prisms (Fig. 4). Regarding forsterite phase, its proportion in the glass-ceramic is almost constant as indicated by the comparable percentage of forsterite at 800, 900 and 1000 °C. From FESEM observations it is possible to note that the microstructure of the glass-ceramic obtained at 900 °C is well-organized and the forsterite

crystals are embedded on the glassy phase; this fact can reduce the close porosity (~9%) and consequently improve the mechanical properties.

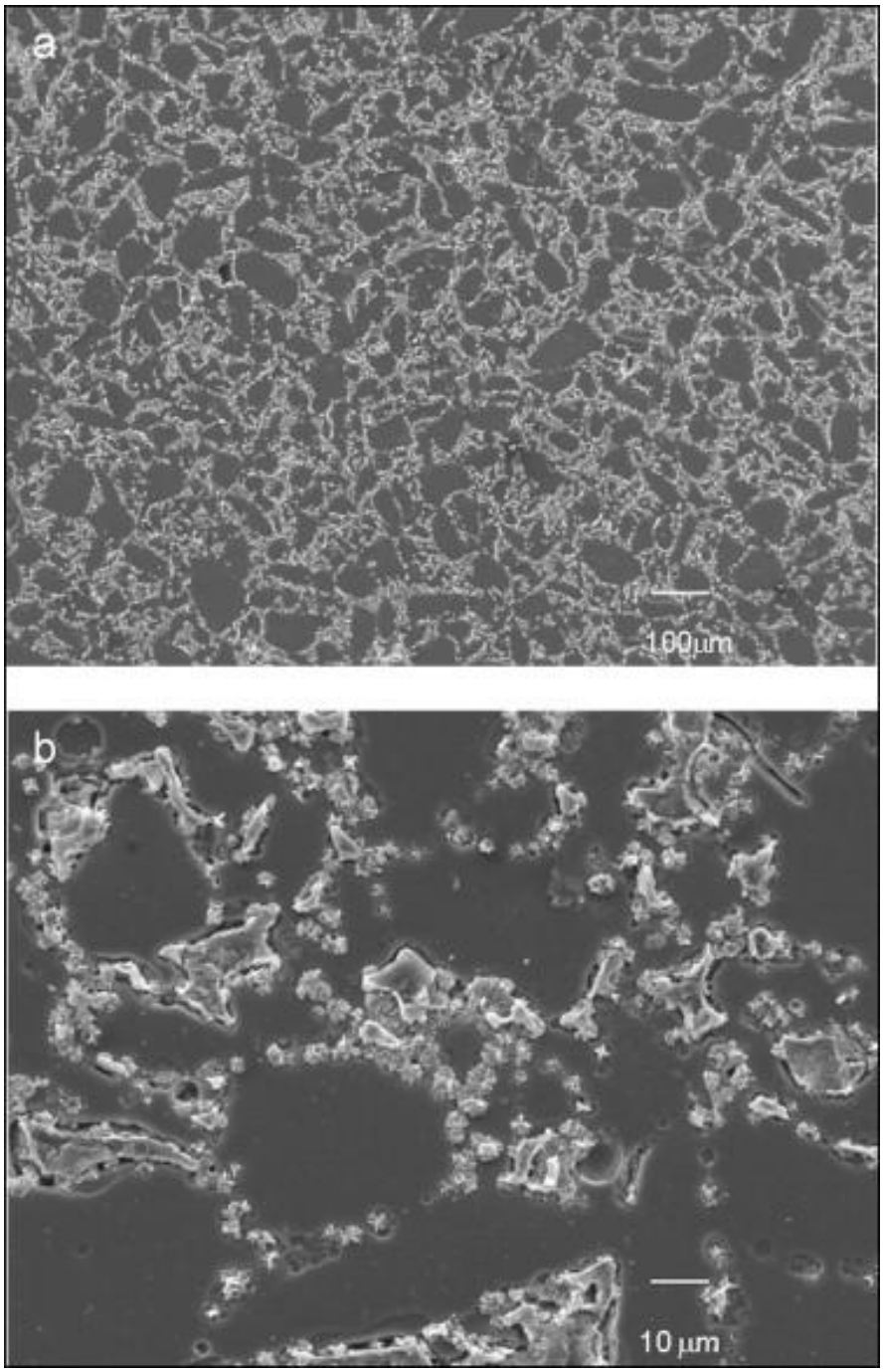

Fig. 2. (a) SEM micrograph (130×) of glass-ceramic treated at 700 °C/40 min; (b) enlargement (800×) of SEM micrograph.

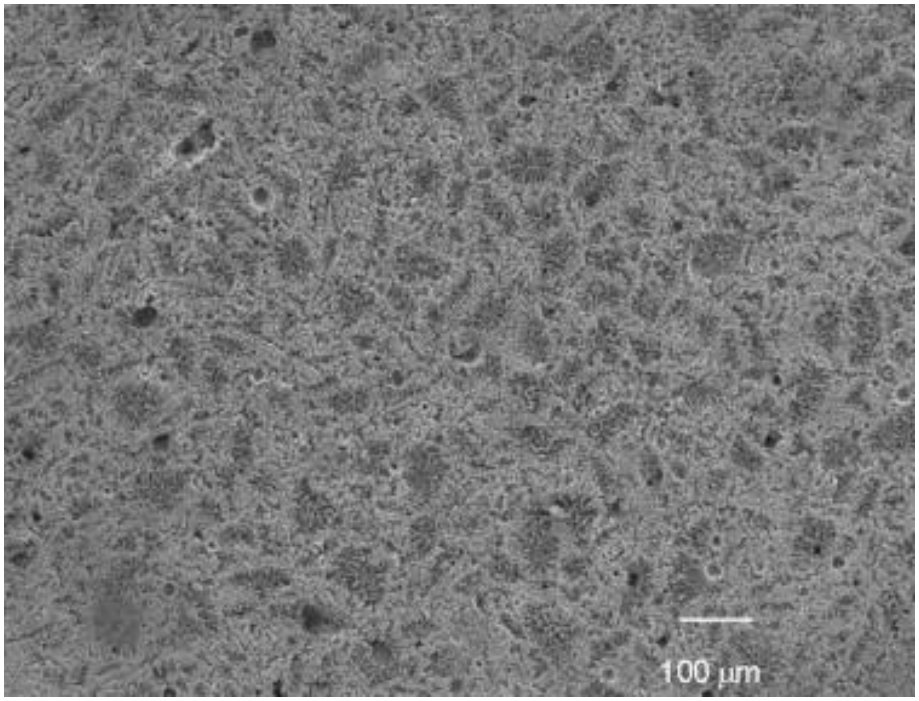

Fig. 3. SEM micrograph of glass-ceramic treated at 800 °C/40 min.

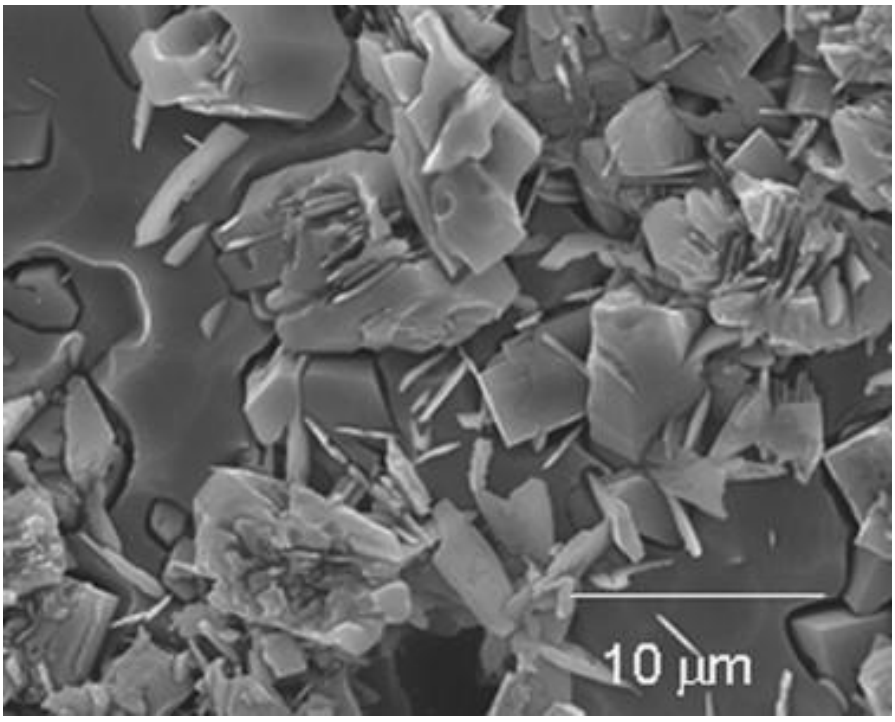

Fig. 4. SEM micrograph of glass-ceramic treated at 900 °C/40 min.

F. Andreola, M.I. Martín, A.M. Ferrari, I. Lancellotti, F Bondioli, J.Ma. Rincón, M. Romero, L. Barbieri, Technological properties of glass-ceramic tiles obtained using rice husk ash as silica precursor. *Ceramics International* Volume 39, Issue 5, July 2013, Pages 5427–5435; doi:10.1016/j.ceramint.2012.12.050

Finally, in order to evaluate the chemical resistance of the glass-ceramics, durability tests in distilled water were conducted. In Table 5 it is possible to observe the results expressed as the amount (μg/g) of the released alkaline ions. The sample heat-treated at 900 °C for 40 min shows the best resistance, followed by parent glass. In contrast the glass-ceramic obtained after a treatment at 750 °C/40 min exhibits the worst worse resistance. This behavior can be explained by considering that nepheline formation removes three moles of glass network-forming oxides (Al_2O_3 and 2SiO per each mole of Na_2O) and it can result in deterioration of the chemical durability of the glass-ceramic [47]. The decrease of nepheline amount for higher temperature and the increase of forsterite, which does not contain alkaline elements, can improve the chemical resistance with respect to also parent glass.

Table 5. Durability in bi-distilled water (95 °C) for both glass-ceramics obtained at different temperatures (soaking time 40 min) and parent glass, expressed as amount release of alkaline ions (μg/g), and their classification (Class 1=very high resistance, Class=2 high resistance, Class=3 medium resistance, Class=4 low resistance).

Temperature (°C)	Alkali leached (μg/g)	Class
750	355	4
900	80.9	3
Parent glass	89.0	3

The crystallization of sodium aluminosilicates such as nepheline in glass-ceramics was observed in literature to depend on their boron content.

The presence of B_2O_3 seems to inhibit the formation of any Na–Al–Si–O based crystalline phase. This role of B_2O_3 in retarding the nepheline formation in glasses can be attributed to its tendency to induce phase separation in these glasses. Since, alkali and alkaline-earth cations have higher affinity for borate-rich component in borosilicate glasses, increasing boron concentration in these glasses strips off the modifier cations from the silicate glass network, inducing re-polymerization and stabilizing the amorphous phase [48]. In this context to have an improvement of the chemical resistance of both parent glass and glass-ceramics an increase of the amount of boron and/or a decrease of sodium can be tailored.

4. Conclusions

The results obtained in this study confirm the possibility to use rice husk ash as silica precursor for the development of nepheline–fosterite glass ceramics. The materials obtained by a thermal treatment at 900 °C for 40 min showed density values similar to the nepheline density reported in literature. The presence of high amount of nepheline causes medium chemical resistance of glass-ceramic, so a correction in the formulation of the materials can be useful. Rietveld R.I.R analysis shows that for this sample the nepheline is the main crystalline phase (43 wt%) with a 11 wt% of fosterite and a great amount of glassy phase (46%). Regarding technological features, the sintered materials showed similar bending strength values and Mohs hardness higher than the commercial glass-ceramics like Neoparies®. Other property as water absorption (≤0.5%) allowed to classify these materials into the Group BIa characteristic of high sintered ceramic tiles according to European Standard rule.

Regarding environmental point of view, significant benefits are attained by using RHA instead of silica: (a) avoided landfill disposal of the residue; (b) minimization of the natural raw materials consumption. Considering that the RHA is not a hazardous residue, the obtained materials do not cause further pollution.

Acknowledgments

Dr. M.I. Martín expresses her gratitude to the Spanish National Research Council (CSIC) for her contract through the JAE Program (JAEDoc-08-00032), co-financed by the European Social Fund.

References

[1] Report of International Rice Research Institute.[http://www.knowledgebank.irri.org/rkb/rice-milling/byproducts-and-their-utilization/rice-husk.html], 2009.

[2] E.C. Beagle. Rice Husk Conversion to Energy. FAO Agricultural services Bulletin, Rome (I) (1978)

[3] L. Velupillai, D.B. Mahin, J.W. Warshaw, E.J. Wailes, A study of the market for rice husk-to-energy systems and equipment. Ed. Louisiana State University Agricultural Center, USA, 1997

[4] J.L. Martin, The Densification of Rice Hulls and a Study of the Products Obtained, MS Thesis, Louisiana State University, Eunice, LA, May, 1938.

[5] G.C. Cordeiro, R.D. Toledo, E.D.R. Fairbairn. Use of ultrafine rice husk ash with high-carbon content as pozzolan in high performance concrete. Materials and Structures, 42 (2009), pp. 983–992

[6] B.K. Ngun, H. Mohamad, E. Sakai, Z.A. Ahmad. Effect of rice husk ash and silica fume in ternary system on the properties of blended cement paste and concrete. Journal of Ceramic Processing Research, 11 (2010), pp. 311–315

[7] C.S. Prasad, K.N. Maiti, R. Venugopal. Effect of substitution of quartz by rice husk ash and silica fume on the properties of whiteware compositions. Ceramics International, 29 (8) (2003), pp. 907–914

[8] F. Andreola, L. Barbieri, F. Bondioli, A.M. Ferrari, T. Manfredini, Valorization of rice husk ash as secondary raw material in the ceramic industry, in: Proceedings of the 10th International Conference of European Ceramic Society (ECERS), Baden-Baden, Germany, 1794–1798, 2007. ISBN: 3-87264-022-4.

[9] M.K. Naskar, M. Chatterjee.A novel process for the synthesis of cordierite ($Mg_2Al_4Si_5O_{18}$) powders from rice husk ash and other sources of silica and their comparative study. Journal of the European Ceramic Society, 24 (13) (2004), pp. 3499–3508

[10] F. Bondioli, F. Andreola, L. Barbieri, T. Manfredini, A.M. Ferrari. Effect of rice husk ash (RHA) in the synthesis of (Pr,Zr)SiO_4 ceramic pigment. Journal of the European Ceramic Society, 27 (2007), pp. 3483–3488

[11] F. Andreola, L. Barbieri, F. Bondioli. Agricultural waste in the synthesis of coral ceramic pigment. Dyes and Pigments, 94 (2012), pp. 207–211

[12] D. Wattanasiriwech, N. Polpuak, P. Danthaisong, S. Wattanasiriwech. Use of rice husk ash for quartz substitution in stoneware glazes. Journal of Scientific and Industrial Research, 67 (6) (2008), pp. 455–460

[13] F. Bondioli, L. Barbieri, A.M. Ferrari, T. Manfredini. Characterization of rice husk ash and its recycling as quartz substitute for the production of ceramic glazes. Journal of the American Ceramic Society, 93 (1) (2010), pp. 121–126

[14] M.K. Naskar, M. Chatteljee. A novel process for the synthesis of lithium aluminum silicate powders from rice husk ash and other water-based precursor materials. Materials Letters, 59 (8–9) (2005), pp. 998–1003

[15] J.F. Mac Dowell. Microwave heating of nepheline glass-ceramics. Journal of the American Ceramic Society, 58 (1975), pp. 258–259

[16] M.C. Wang, N.C. Wu, M.H. Hon. Preparation of nepheline glass-ceramics and their application as dental porcelain. Materials Chemistry and Physics, 37 (1994), pp. 370–375

[17] E.M.A. Hamzawy, E.M. El-Meliegy. Preparation of nepheline glass-ceramics for dental applications.Materials Chemistry and Physics, 112 (2008), pp. 432–435

[18] E.M.A. Hamzawy, E.M. El-Meliegy. Crystallization in the Na_2O–CaO–Al_2O_3–SiO_2–(LiF) glass compositions. Ceramics International, 33 (2007), pp. 227–231

[19] E.M.A. Hamzawy, C. Leonelli. Crystallization, microstructure and expansitivity of apodumene-nepheline glasses. Glass Science and Technology, 77 (2004), pp. 289–294

[20] E.I. Suzdal'tsev, D.V. Kharitonov, A.A. Anashkina. Analysis of existing radioparent refractory materials, composites and technology for creating high-speed rocket radomes. Part 4. Ceramic technology for producing glass ceramic radomes. Advantages and disadvantages. Prospects for modernization. Refractories and Industrial Ceramics, 51 (2011), pp. 349–357

[21] M. Romero, M. Kovacova, J.Ma. Rincón. Effect of particle size on kinetics crystallization of an iron-rich glass. Journal of Materials Science, 43 (2008), pp. 4135–4142

[22] M.S. Hernandez-Crespo, M. Romero, J.Ma. Rincon. Nucleation and crystal growth of glasses produced by a generic plasma arc-process. Journal of the European Ceramic Society, 26 (2006), pp. 1679–1685

[23] M.S. Hernandez-Crespo, M. Romero, J.Ma. Rincon. Leaching behavior of a glassy slag and derived glass ceramics from arc plasma vetrification of hospital wastes. Advances In Applied Ceramics, 108 (2009), pp. 67–71

[24] N. Kanchanarat, S. Bandyopadhyay-Ghosh, I.M. Reaney, I.M. Brook, P.V. Hatton. Microstructure and mechanical properties of fluorcanasite glass-ceramics for biomedical applications. Journal of Materials Science, 43 (2008), pp. 759–765

[25] R. Casasola, J.Ma. Rincón, M. Romero. Glass-ceramic glazes for ceramic tiles—a review. Journal of Materials Science, 47 (2012), pp. 553–582

[26] M. Pelino Recycling of zinc-hydrometallurgy wastes in glass and glass ceramic materials. Waste Management, 20 (7) (2000), pp. 561–568

[27] F.A. López, M.I. Martín, F.J. Alguacil, J.Ma. Rincón, T.A. Centeno, M. Romero. Thermolysis of fibreglass polyester composite and reutilisation of the glass fibre residue to

obtain a glass-ceramic material. Journal of Analytical and Applied Pyrolysis, 93 (2012), pp. 104–112

[28] E. Mustafa, N. Khalil, A. Gamal. Sintering and microstructure of spinel-forsterite bodies. Ceramics International, 28 (2002), pp. 663–667

[29] T.S. Sasikala, M.N. Suma, P. Mohanan, C. Pavithran, M.T. Sebastian. Forsterite-based ceramic-glass composites for substrate applications in microwave and millimeter wave communications. Journal of Alloys and Compounds, 461 (2008), pp. 555–559

[30] Y. Demirci, E. Günay. Crystallization behavior and properties of cordierite glass-ceramics with added boron oxide. Journal of Ceramic Processing Research (2001), pp. 352–356

[31] M.I. Martín, M. Romero, J.Ma. Rincon, F. Andreola, L. Barbieri, F. Bondioli, I. Lancellotti. Materiales vitrocerámicos del sistema MgO–Al2O3–SiO2 a partir de ceniza de cáscara de arroz. Boletin de la Sociedad Española de Ceràmica y Vidrio, 50 (2011), pp. 201–206

[32] A.C. Larson, R.B. Von Dreele. General structure analysis system (GSAS). Los Alamos National Laboratory Report LAUR (2000), pp. 86–748

[33] B.H. Toby EXPGUI, a graphical user interface for GSAS. Journal of Applied Crystallography, 34 (2001), pp. 210–213

[34] Official Web Site Micromeritics, 〈http://www.micromeritics.com〉.

[35] K. Heritage, C. Frisby, M. Wolfender. Impulse excitation technique for dynamic flexural measurements at moderate temperatura. Review of scientific instruments, 59 (1988), pp. 973–974

[36] ISO 10545-6:2010. Ceramic Tiles Part 6. Determination of resistance to deep abrasion for unglazed tiles, 2010.

[37] D.M. Ibrahim. Crystallite growth of rice husk ash silica. Thermochimica Acta, 45 (1981), pp. 79–85

[38] D.M. Ibrahim, S.A. El-Hemaly, F.M. Abdel-Kerim. Study of rice husk ash silica by infrared spectroscopy. Thermochimica Acta, 37 (1980), pp. 307–314

[39] O.W. Floerke. The crystalline forms of SiO2 and their transformation behavior. Berichte der Deutschen Keramischen Gesellschaft, 38 (3) (1961), pp. 89–91

[40] 〈http://www.negb.co.jp/en/product/01/01.html〉 (retrieved July, 2012).

[41] EN ISO 10545-3. Ceramic tiles. Part. 3. Determination of water absorption, apparent porosity, apparent relative density and bulk density.

[42] P. Appendino, M. Ferraris, I. Matekovits, M. Salvo. Production of glass-ceramic bodies from the bottom ashes of municipal solid waste incinerators. Journal of the European Ceramic Society, 24 (5) (2004), pp. 803–810

[43] A.D. Papargyris, R.D. Cooke. Structure and mechanical properties of kaolin based ceramics. British Ceramic Transactions, 95 (3) (1996), pp. 107–120

[44] D.N. Boccaccini, A.R. Boccaccini. Dependence of ultrasonic velocity on porosity and pore shape in sintered materials. Journal of Nondestructive Evaluation, 16 (1997), pp. 187–192

[45] H. Gercek. Poisson's ratio values for rocks. International Journal of Rock Mechanics and Mining Sciences, 44 (1) (2007), pp. 1–13

[46] W. Hölland, G. Beall. Glass-Ceramic Technology. The American Ceramic Society, Ohio (2002)

[47] H. Li, J.D. Vienna, P. Hrma, D.E. Smith, M.J. Schweiger. Nepheline precipitation in high-level waste glasses: compositional effect and impact on waste form acceptability. Materials Research Society Symposia proceedings, 465 (1997), pp. 261–268

[48] G. Ashutosh, J.S. McCloy, K.M. Fox, C.J. Leslie, B.J. Riley, C.P. Rodriguez, M.J. Schweiger. Structural analysis of some sodium and alumina rich high-level nuclear waste glasses. Journal of Non-Crystalline Solids, 358 (3) (2012), pp. 674–679